ICAMMP 2011 International Conference on Advances in Materials and Materials Processing, Indian Institute of Technology Kharagpur, 9-11 December, 2011

Study of 'gold black' coating as potential thin film solar cell efficiency enhancer

Deep Panjwani[a], Christopher J. Fredricksen[b], Samuel J. Peppernick[c], Alan G. Joly[c], Kenneth M. Beck[c], Yauheni Rudzevich[a] Robert E. Peale[a]

[a]Department of Physics, University of Central Florida, Orlando FL 32816
[b]LRC Engineering Inc, 9345 Chandon Dr., Orlando, FL 32825
[c]Pacific Northwest National Laboratory, P.O. Box 999, Richland, WA 99352, USA

ABSTRACT

Efficiency enhancement of thin film solar cells was obtained using deposited gold-black particles as scattering centers. Gold black is shown to give a broad particle size distribution from nm to several microns. This results in plasma resonance-enhanced scattering and intensified local electric field over a broad spectrum. Initial experiments on thin film solar cells with gold black showed an increase in short-circuit photocurrent 20% in the 350 to 1000 nm spectral range and an increase in the efficiency of 7%. Photoemission electron microscopy (PEEM) reveals the spectral and spatial distribution of plasmon resonances for gold black using UV, visible, and near IR wavelength sources. Plasma resonances occur out to at least 800 nm wavelength, as evidenced by localized regions of high photoemission.

Keywords: thin film solar cell, localized surface plasmons, gold black, nano materials

INTRODUCTION

For future energy needs, the cost of the photovoltaic technology must compete favorably with conventional electricity production. Presently, the solar-cell market is dominated by crystalline silicon cells of at least hundred micron thickness, giving reasonable performance but at high material costs. Thin film cells promise cost reductions with absorber layers as thin as 1 micron. However, at this thickness the absorber is partially transparent and incapable of harvesting the entire solar flux. Therefore, engineered light trapping is of interest to improve efficiency [1,2].

Many are investigating front surface depositions of nanoparticles, which serve as scattering centers to increase the effective optical path length within the absorber layer. Scattering is enhanced at the plasma resonance frequency, which depends on the size and material of the particle and the surrounding dielectric[3,4]. Furthermore, the strong interaction of light and nanoparticles at resonance enhances the near field, potentially resulting in stronger absorption. Electrodynamic simulation of 100 nm gold spheres has demonstrated the effects of near-field enhancement and channeling of radiation inside the silicon absorber layer [5]. Lithographically produced or self-assembled arrays of nano particles have increased photocurrent, but not for entire solar spectrum due to limited size dispersion. It remains a challenge to optimize the particle size and pitch to ensure the enhanced scattering over the entire useable solar spectrum [3,4].

Gold blacks, a nano-structured material with broad feature size distribution, can be produced cheaply in a low-vacuum process, requiring no lithographic patterning. Thus, gold black provides opportunity to harvest the entire solar flux. The particle size, packing fraction, and nature of aggregation of gold particles can be controlled with the deposition parameters such as inert gas pressure, deposition rate, and the mass of the gold in the boat [6-10].

MATERIALS AND EXPERIMENTAL DETAILS

Thin and sparse gold black films were deposited on thin film solar cells in a thermal evaporator back-filled with ~1 Torr N_2. The cell and piece of silicon substrate were mounted side-by-side on a temperature-controlled, thermoelectrically-cooled, copper block. In presence of N_2, evaporated gold particles, combine into nano-scale agglomerates, diffuse towards the cooler substrate, and are deposited on the surface to form a web-like structure with a broad range of feature sizes. The Si substrate, with cm^2 area, allowed characterization of the deposited films by various microscopies.

Before the deposition, the chamber pressure is pumped below 10^{-4} Torr, and then back filled with N_2 to the desired pressure. The thermoelectric cooler cools the substrate to ~0 C. The appropriate current is passed through the Mo boat containing gold to achieve the desired deposition rate. After the deposition the substrate is brought to the room temperature before venting the chamber to avoid condensation of moisture.

Harris showed that lower deposition rate provides a wider range of particle sizes [11]. We found that very low boat currents, such that reaching gold melting point took 2 hours, resulted in heavy contamination by Mo, as determined by energy dispersive spectroscopy (EDS) in an electron microscope. To avoid this, we started with high boat currents to quickly reach the melting temperature of the gold. As soon as the gold load was drawn into a sphere by surface tension and before it wet and flowed over the boat surface, the current was abruptly dropped to lower the deposition rate. By this means we obtained an open web structure with a broad distribution of length scales and minimal Mo contamination.

Net photovoltaic conversion efficiency with & without gold-black depositions was measured using the apparatus presented in Fig. 1. For broadband solar-simulated illumination, a Xenon arc lamp with AM 0 and AM 1.5 filters was used, which in the Fig. 1 (left) configuration irradiated the cell with 350 mW over a 50 mm diameter spot, which is 13% of one sun. A monochromator (Fig. 1, right) was used to obtain the spectral photo response in range of 350 to 1100 nm, with data recorded and displayed in Labview.

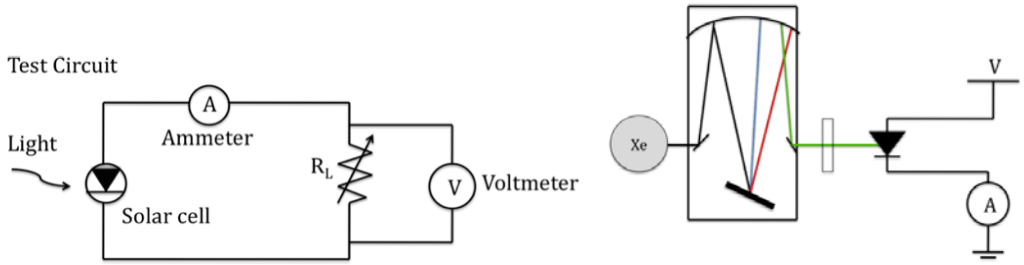

Fig.1 (left) Schematic of set-up for characterizing solar cell IV curves. A given current is passed through the solar cell and the voltage across the cell is measured using a variable load resistance, a measurement facilitated by use of a Keithley source-meter. (right) Schematic of spectral response set-up. Monochromated Xe arc lamp light of calibrated intensity passes through a filter to remove harmonics and impinges on the solar cell, whose IV curve is measured.

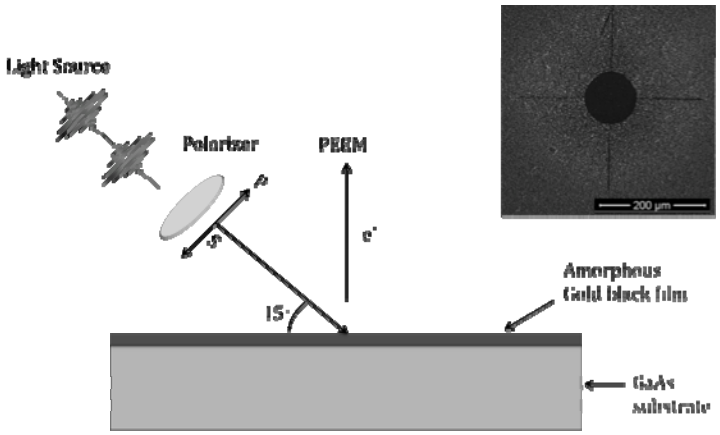

Fig. 2 Experimental PEEM Setup. The inset shows gold black sample with registration mark prepared using FIB.

Photoemission electron microscopy (PEEM) was performed at the Environmental Molecular Sciences Lab of Pacific Northwest National Lab in Richland Washington, see Fig. 2. PEEM images photo-emitted electrons. The image contrast depends on the work function of the material under the study [12], but resonance enhancement of local electric fields can lead to enhanced photoemission even at photon energies below the work function. Emitted electrons transmit through electron optics before striking a phosphor screen, where the image is then captured by a charged coupled device (CCD). An unpolarized mercury

discharge lamp (EQ 1500), with a peak in its broad spectrum at 4.9 eV, was used one source used for PEEM. With this source, it is not generally possible to see photoemission from bulk Ru with work function 5.3 eV, but Cu with work function 4.6 eV easily appears. By the same token, bulk gold with work function 5.1 eV, would not have significant photoemission using this Hg lamp. Next, PEEM images were acquired using femtosecond pulses of Titanium Sapphire laser with wavelengths 400 or 800 nm. The laser polarization vector could be controlled by a rotating waveplate, though no polarization dependent results are reported here. The laser beam was incident on surface at 15^{o} angle with respect to the sample surface, as shown in Figure 2. The laser spot illuminates the surface of the sample in elliptical area with major axis of 100 μm and minor axis of 30 μm. To correlate PEEM images with other microscopies, alignment marks were made by Focused Ion Beam (FIB) milling, as shown in the Fig. 2 inset.

Scanning and Transmission Electron Microscopies (SEM and TEM, respectively) were performed in the Materials Characterization Facility at UCF. Fractional coverage of the surface by gold black particles was determined from histograms of the SEM images as the ratio of bright pixels (gold-black) to the total number of pixels. The dark part of the histogram corresponds to the silicon substrate, while bright shoulder extending over 100-pixel brightness is due to gold black particles. Wavelet analysis has proven useful to quantify the size distribution [5].

RESULTS

As suggested by the Figure 3 (left) micrograph, the density of gold black films is very low, simultaneously providing metallic scattering centers and open windows to the solar cell surface. A TEM image of a similarly prepared sample is presented in Fig. 3 (right) and shows the web-like structure of gold-black with feature sizes ranging from a few nm to microns. The smallest length scales are more evident in the high resolution TEM image of Fig. 4. Electron diffraction patterns have shown that orientations are random and only the pure gold is present in ideal depositions [11].

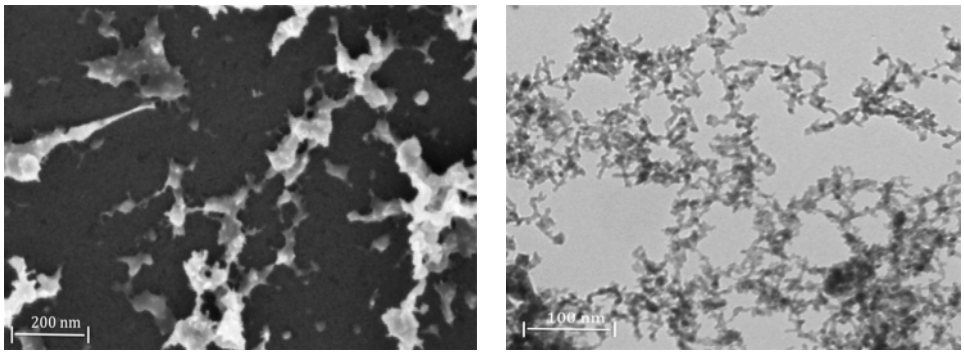

Fig. 3 (left) Scanning electron microscopy (SEM) on gold black sample, showing feature sizes from 10 to 500 nm. The boat load was less than 0.2 mg and the inert gas pressure was 400 mTorr. (right) Transmission electron microscopy (TEM) on similar gold black sample reveals more of the fine structured component.

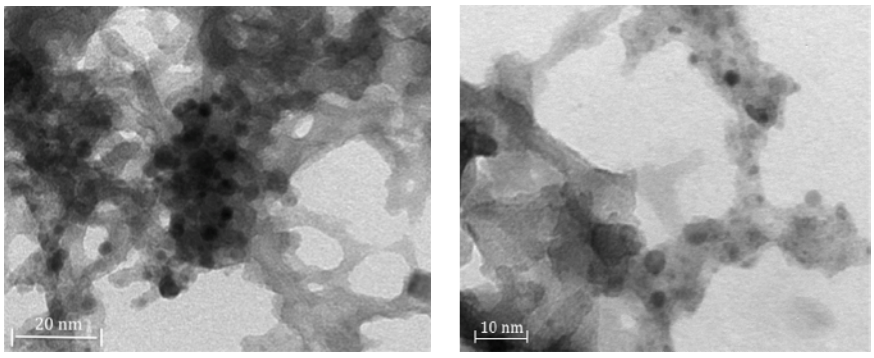

Fig. 4 High resolution TEM image showing nano structure of gold black. Scale bars are (left) 20 nm and (right) 10 nm.

Histograms for lightly and heavily coated samples are presented in Fig. 5. These show that the percent coverage can be quantified. This is useful for correlating this figure of merit with changes in solar cell efficiency.

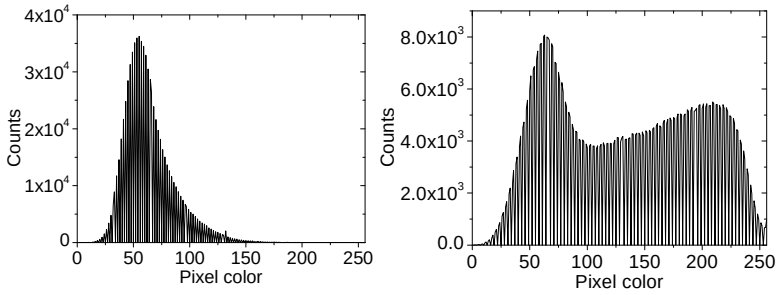

Fig. 5 Histograms of SEM images for light- (left) and heavy- (right) coatings of gold black on silicon substrate. Deposition parameters were {0.5 mg Au, 400 mTorr, 68 A} and {1.5 mg Au, 1000 mTorr, 68 A}, respectively.

Fig. 6 (left) demonstrates a post-deposition photocurrent increase of ~20% at most wavelengths, while the improvement was less (~10%) at the peak of the photo response at 580 nm. This spectral dependence is understandable, since the improvement caused by scattering should be strongest at those wavelengths where the absorption by the film alone is weakest. The improvement disappeared when the deposited metal particles were wiped off. Since we removed the gold black coating from this sample, another sample was used for broad band experiments. Fig. 6 (right) shows its I-V before and after deposition, demonstrating a 7% efficiency increase, but since we lost the sample we could not measure the photo current response, even though the improvement in (I_{sc}) in this case was much less than for Fig. 6 (right).

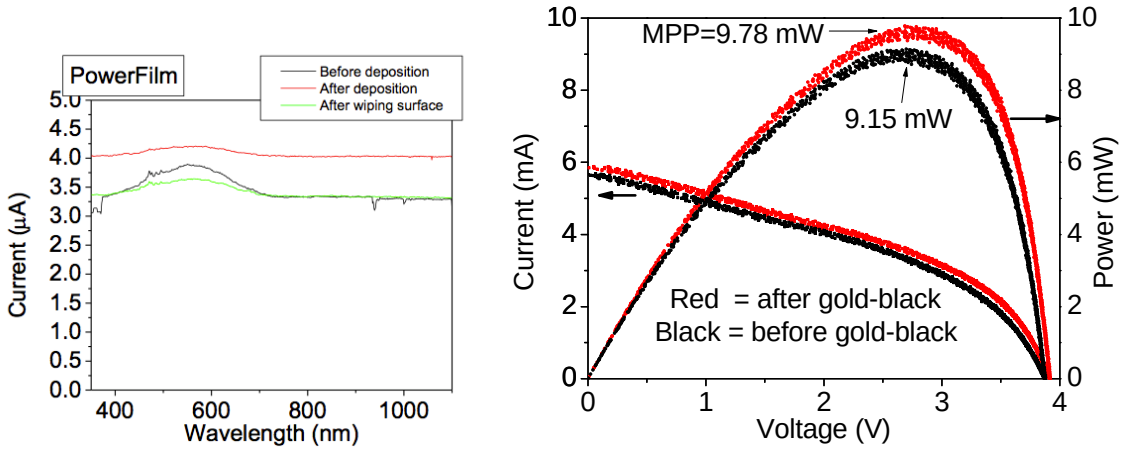

Fig. 6 (left) Demonstration of short-circuit photocurrent increase across the spectrum for thin film solar cell coated with gold-black particles. From the I-V curve (right), the maximum power point (MPP) before deposition was 9.15 mW, which increased by 7% after deposition.

We performed PEEM analysis on a gold-black sample, where the region of the sample studied is indicated by the FIB alignment mark in the SEM image of Fig. 7 (left). In the case of a heterogeneous specimen such as gold black deposited on Si substrate, areas with low photoelectron yield appear darker. Localized surface plasmon resonances assist in photoemission due to local field enhancement, so such resonances are identified by high levels of photoemission, even when the photon energy is below the work function of the bulk material. Fig. 7 (right) presents the PEEM image of the sample using the Hg lamp for excitation. The direction of incidence is shown by the arrow on the upper left outside the field of view. Even though most of the photon energies for the Hg lamp spectrum are less than the work function of bulk gold (5.1 eV), we see photoemission from most of the gold-black particles. The particles plowed up by the FIB marking process are the brightest features in the image.

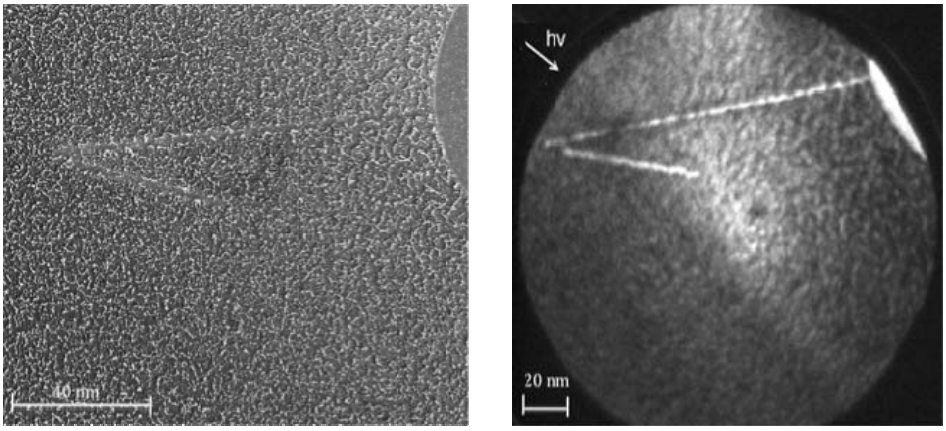

Fig. 7 (left) SEM image of the gold black sample under study with FIB alignment mark. (Right) PEEM image of the sample taken using unpolarized Hg lamp and an integration time of 0.1 s

High photoemission across the sample is still seen when illuminated with 400 nm laser light, as shown in Figure 8 (left). The corresponding photon energy of ~3.10 eV falls below the 5.1 eV work function of bulk gold, but it is above its ~2.5 eV plasma frequency. The PEEM image is very bright, and a portion of the FIB alignment mark is visible as dark lines. This is in contrast to Fig. 7 (right), where the same alignment mark is the brightest feature.

Figure 8 (right) present a PEEM image from gold-black samples using 800 nm wavelength excitation. The photon energy 1.55 eV is twice lower, even farther below the gold work function, than in Fig. 8 (left), and it is also well below the ~2.5 eV plasma frequency for bulk gold. The photoemission bright spots are observed to be far fewer, though they still occur. This observation holds even though the incident power is 12.5 x higher and the integration time 5 x times higher (note the brighter background), while at a given wavelength, the photoemission electron yield would be expected to be proportional to the square of the laser intensity [14]. In Fig. 8 (right) there is no longer any trace of the alignment mark, even though the area of illumination was unchanged from that of Fig. 8 (left).

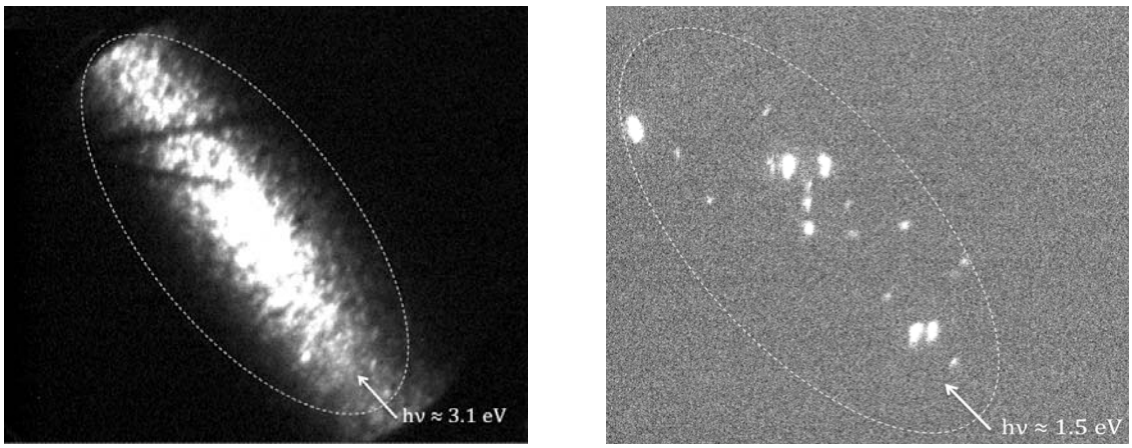

Fig. 8 PEEM images with 150 micron FOV. (left) fs laser excitation at 400 nm wavelength, 12 mW power, and 0.1 s integration time (right). fs laser excitation at 800 nm wavelength, 150 mW power, and 0.5 s integration time. The dotted contour indicates the illuminated spot on the sample.

CONCLUSIONS AND DISCUSSION

Gold black deposition on thin film solar cells results in a clear efficiency enhancement. Advantages of this approach include ease of production and an inherently broad particle size from nm to

micron, as shown by SEM and TEM microscopy. Thus, a broad range of scattering and field enhancing plasma resonances are expected across the entire solar flux.

To summarize the PEEM results, the main factor in obtaining high photoemission electron yield appears to be having sufficiently high photon energy. Yet, it is remarkable that spots of high photoemission still occur (though fewer) at photon energies that are well below both the bulk work function and the plasma frequency. We note that PEEM analysis on silver nano particles of 232 nm size also showed high near-field enhancement at photon energies below the bulk plasma frequency (~ 3.7 eV) [13]. We interpret this observation as the action of plasma resonances which are pushed to lower frequencies by particle size effects.

The spatial distribution of plasma resonances is expected to change with wavelength throughout the solar spectrum. Our PEEM observations span that spectrum, showing that resonances extend from near UV to the far end of the useful solar spectrum near 800 nm. It is in principle possible to optimize the parameters of deposition providing a suitable density of resonant particles over a broad spectral range throughout the solar range.

Electrodynamic simulations have potential to model the intensity and scattering profiles inside solar cell absorber layer with different morphologies for the gold-black layer. Correlation of deposition parameters with wavelet and percentage coverage analysis will then aid the optimization of the gold-black coating for maximum efficiency enhancement.

REFERENCES

[1] Atwater H. and Polman.A. Nature Mater 2010; 205-9.
[2] Pillai S. & Green M.A. Solar energy Materials & Solar Cells 2010: 94 1481-1486.
[3] Catchpole K.R. and Polman A. Applied. Phys. Letter 2008: 94 191113.
[4] Catchpole K.R. Trans Phill. R. Soc 2006: A 364, 3493-3503.
[5] Panjwani D, Peale R, Oladeji I, Khalilzadeh F, Baillie K, Colwell J, Fredricksen C. SPIE Proceeding 2011: Volume 3. 8035 – 25.
[6] Harris L, McGinnies R.T. and Siegel B.M. Journal of Optical Society 1948: 38, 582-589.
[7] Harris L and Beasley J.K. J. Opt. Soc. 1952 Am. 42, 134-140.
[8] Harris L and Loeb A.L. J. Opt. Soc. 1953 Am. 43, 1114-1118.
[9] Harris L. J. Opt. Soc 1961: Am. 51, 80-82.
[10] Harris L and Fowler P. J. Opt. Soc. 1961 Am. 51, 164-167.
[11] Harris L and Jeffries D. Journal of Applied Physics 1948, Volume 19, 791-794.
[12] Xiong G, Shao R, Peppernick S.J, Joly A.G, Beck K.M, Hess W. Cai M, Duchene J, Wang J.Y, and Wei W.D. Journal of Materials 2010: 62, 90.
[13] Samuel J. Peppernick S.J, Joly A.G, Beck K.M, Hess W.P, Journal of Chemical Physics 2011 **134**, 034507.
[14] Tsang T, Srinivasan-Rao T and Fischer J. Phys. Rev. B 1991: 43, 8870.